Journal of Materials Chemistry C

Accepted Manuscript

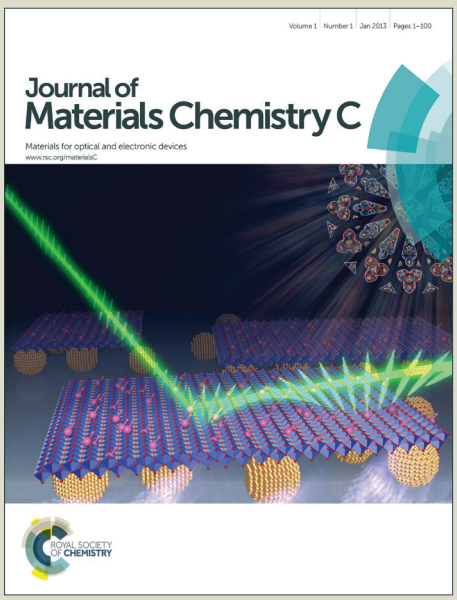

ROYAL SOCIETY OF CHEMISTRY

www.rsc.org/materialsC

Journal of Materials Chemistry C

Cite this: DOI: 10.1039/c0xx00000x

www.rsc.org/xxxxxx

PAPER

Switch the triplet excited state of the C_{60}-dimethylaminostyryl bodipy dyads/triads

Ling Huang and Jianzhang Zhao*

Received (in XXX, XXX) Xth XXXXXXXXX 20XX, Accepted Xth XXXXXXXXX 20XX

DOI: 10.1039/b000000x

In order to switch the triplet excited states in organic compounds, dimethylaminostyryl Bodipy-C_{60} dyads and triads were prepared. The triplet excited states of the compounds were switched with acid/base, the mechanism was studied with nanosecond time-resolved transient difference absorption spectroscopy. The visible light-harvesting Bodipy antennas are the electron or singlet energy donor, whereas C_{60} moiety is the electron/singlet energy acceptor, as well as the spin converter to produce triplet excited states. Our strategy of triplet state switching is to control either the photoinduced electron transfer (PET) or the singlet state energy transfer (EnT) from the antenna to C_{60} moiety, by protonation of the dimethylamino styryl Bodipy unit. Population of the triplet state was observed for the dyads with mono(4-dimethylaminostyryl) substituents on Bodipy antenna in nonpolar solvent such as toluene (τ_T = 168.6 μs). Formation of the charge transfer state (CTS) in polar solvent quenches the triplet excited state (τ_T < 10 ns). In the presence of acid, the dimethylaminostyryl Bodipy moiety is protonated, thus the electron transfer (ET) was inhibited. The cascade acid-activated EnT and the intersystem crossing (ISC) of C_{60} produce the triplet excited state. For the dyad and the triads with bis(4-dimethylaminostyryl) substituents on Bodipy antenna, the antenna S_1 state energy level is lower than the S_1 state energy level of C_{60}, thus no EnT to C_{60} exist, and no triplet state was produced upon selectively excitation into the Bodipy moiety. With protontation of the aminostyryl substituents, the S_1 state energy level of the antenna is promoted to be higher than S_1 state of C_{60} moiety, as a result EnT is activated and triplet state is produced. In all the compounds the triplet excited state is localized on the dimethylaminostyryl Bodipy moiety, not on the C_{60} miety. The triplet state switching was conveyed to the the singlet oxygen ($^1O_2$) photosensitizing ability of the compounds, and the variation of the singlet oxygen quantum yield, Φ_Δ, is from 1.9% to 73%.

Introduction

Triplet photosensitizers are important in photocatalysis,[1-4] molecular devices,[5-6] and more recently in triplet-triplet annihilation upconversion.[7-11] Different from the study of *singlet* excited states, study on *triplet* excited state of organic chromophores is rare.[12] Switching of the *singlet* excited state leads to many applications, such as fluorescent molecular sensors,[13-15] visible light-harvesting molecular arrays, etc.[16-19] The mechanisms for switching of singlet excited states include fluorescence resonance energy transfer (FRET),[13a-13d] photo-induced through-bond energy transfer (TBET),[13e,13f] photoinduced electron transfer (PET) and photoinduced intramolecular charge transfer (ICT), etc.[13g] It is highly desired to develop mothodologies for controling of the positioning of triplet state in a multichromophore molecule.

Previously amino-containing bromo-aza Bodipy was studied as acid-activatable photodynamic theraputic (PDT) reagents.[20] PET mechanism is responsible for the acid-activated OFF and ON state of the photosensitizers to produce triplet excites state, thus the ability to sensitizing singlet oxygen ($^1O_2$). Bodipy dyads were also studied as molecular devices for modulation of triplet state in which the direction of FRET can be controled by addition of acid.[5,6] In these studies, however, the triplet excited state manifolds were not studied in detail with nanosecond time-resolved transient difference absorption spectroscopy.[12] Moreover, it is clear that more switching approaches should be explored for switching of the triplet states in organic compounds.

Herein we studied the switching of triplet excited state of C_{60}-styryl Bodipy dyads/triads by controling either the photoinduced intramolecular electron transfer (ET) or energy transfer (EnT).[13c] In the dyads **B-1** and **B-2**, and the triads **B-3** and **B-4** (Scheme 1-2), the Bodipy moieties are visible light-harvesting antennas and electron donor or singlet energy donor; C_{60} moiety is the electron acceptor and singlet energy acceptor, as well as the intramolecular spin converter.[12] Bodipy moeities show strong absorption of visible light, but the intersystem crossing (ISC) is non-efficient. The contrary is true for C_{60} moiety, i.e. the ISC is efficient (close to unity) but its visible light-absorption is poor. Considering the singlet energy levels of the antenna and C_{60}

moiety, RET is possible for **B-1** and **B-3**, thus triplet excited state can be produced. In **B-2** and **B-4**, however, the S_1 state energy level of the antenna is presumably lower than C_{60}, thus RET is impossible; but the EnT can be activated by protonation. Thus in the presence of acid, triplet state production was observed with **B-2** and **B-4**.

The visible light-harvesting antenna in **B-1** – **B-4** were selected so that either the ET or the EnT to the C_{60} moieties can be switched by acid, i.e. prototnation of aminostyryl Bodipy moiety. The ET and singlet/triplet EnT were investigated with steady state and nanosecond time-resolved spectroscopy, as well as electrochemical studies. For all the dyads and the triads, the T_1 state is localized on the styryl Bodipy moiety, not on C_{60} moeity. This conclusion is based on the nanosecond time-resolved transient difference absorption spectroscopy. We show that the $^1O_2$ production with the dyads can be modulated by addition of acid and base.

Results and Discussions

Molecular design and synthesis

The Bodipy moiety was selected as the visible light-harvesting antenna, due to its excellent photophysical properties, such as strong absorption of visible light, high fluorescene quantum yields (less non-radiative decay of the singlet excited state), and feacsible derivitization.[14,19,21] Aminostyryl Bodipy moiety in **B-2** and **B-4** show lower S_1 state energy level than the C_{60} moiety, thus EnT is impossible in **B-2** and **B-4**.[12,22-27] As a result, population of the triplet excited state in **B-2** and **B-4** will be non-efficient, upon selectivily excited into the Bodipy antenna. In the presence of acid such as trifluoroacetic acid (TFA), however, the amino group will be protonated, thus the S_1 state energy level of the antenna in **B-2** and **B-4** will be promoted,[28] to be higher than that of C_{60}, thus EnT become possible, as a result, triplet excited state will be produced by the protonated **B-2** and **B-4**. For **B-1** and **B-3**, the S_1 state energy level of the Bodipy antenna is higher than that of C_{60}. However, ET to C_{60} may quench the triplet excited state. In the presence of TFA, ET will be inhibited and the RET will be activated, as a result, triplet excited state can be produced by the protonated **B-1** and **B-3**. **B-3** and **B-4** are Bodipy-C_{60} triads, which show broadband absorption in visible region.[29]

The preparation of the visible light-antennas are based on routine derivatization methods of Bodipy.[14,19] Condensation of the Bodipy with 4-dimethylaminobenzenealdyhede gives the Bodipy antenna which show absorption at 600 nm or 700 nm, dependent on the number of the substituents.[30] The Bodipy antenna was linked to C_{60} moiety by the Prato reaction. For triads **B-3** and **B-4**, Suzuki cross coupling reaction was used to prepare the broadband visible light-harvesting antenna and Cu(I)-catalyzed Click reaction was used to link the Bodipy and the dimethylamino styryl Bodipy together.[31,32] All the compounds were obtained in moderate to satisfactory yields.

UV–Vis absorption and fluorescence emission spectra

The UV−Vis absorption of the compounds were studied (Fig. 1). **B-1** shows strong absorption at 622 nm, which is due to the dimethylamino styryl Bodipy moiety. **B-2** shows red-shifted absorption at 712 nm, due to the bis(4'-dimethylaminostyryl)

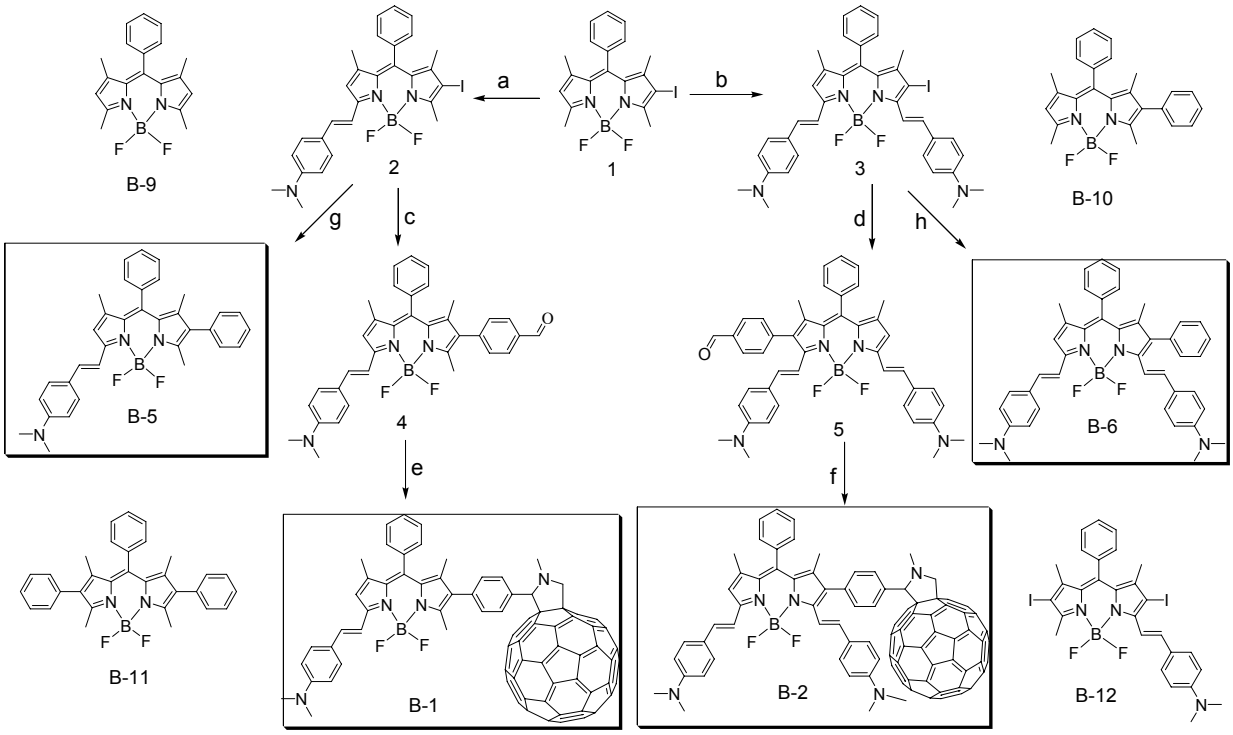

Scheme 1 Synthesis of the C_{60}-dimethylaminostyryl Bodipy dyads **B-1** and **B-2** and the reference compounds. Key: (a) 4–*N,N*–dimethylbenzaldehyde, toluene, acetic acid, piperidine, reflux, 4 h in Ar; (b) the same to (a); (c) 4–formylphenylboronic acid, K_2CO_3, $Pd(PPh_3)_4$; (d) the same to (c); (e) Sarcosine, fullerenes, toluene; reflux; (f) the same to (e); (g) Phenylboronic acid, K_2CO_3, $Pd(PPh_3)_4$; (h) the same to (g).

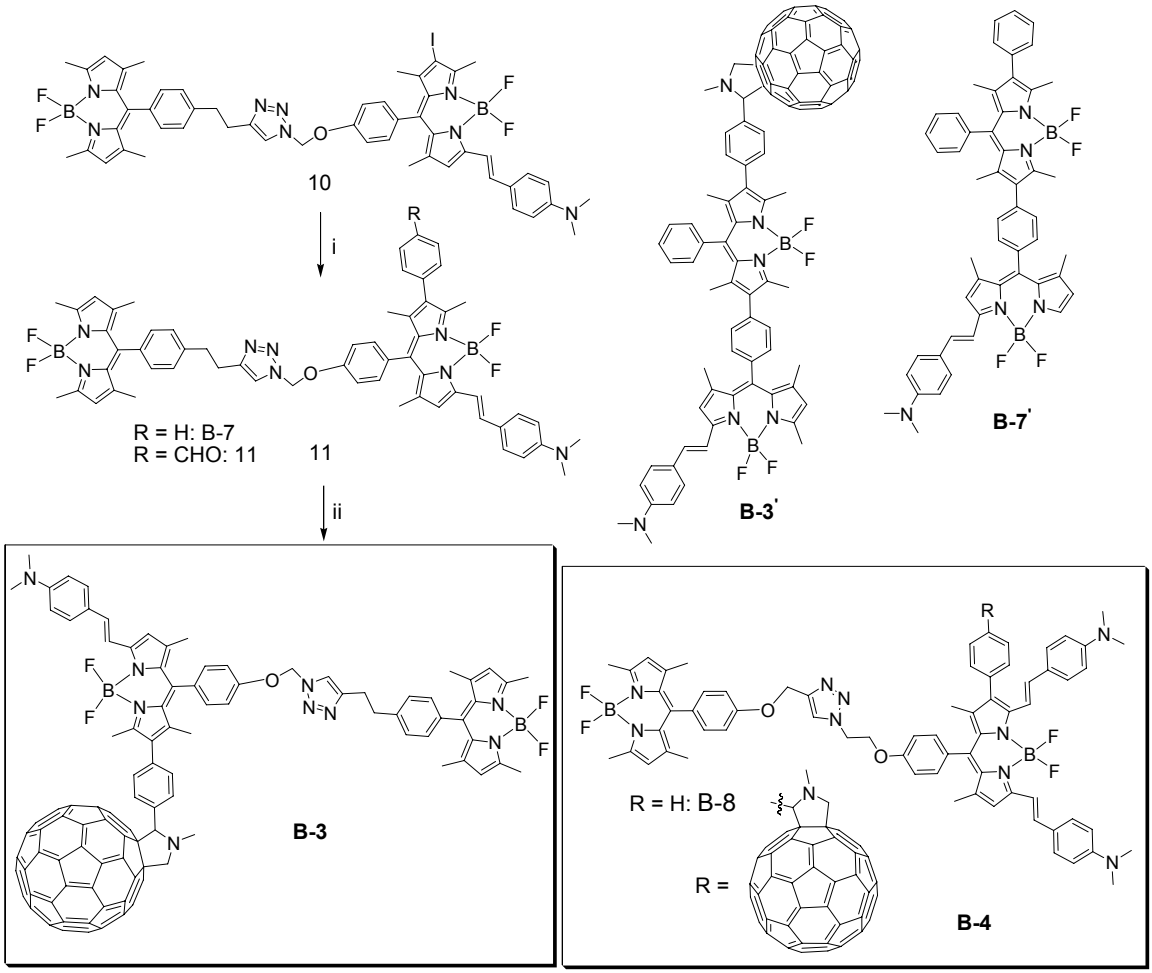

Scheme 2 Synthesis of the C_{60}-dimethylaminostyryl Bodipy triads **B-3** and **B-4** and the reference compounds. (i) Phenylboronic acid, K_2CO_3, $Pd(PPh_3)_4$; (ii) Sarcosine, fullerenes, toluene.

substituted Bodipy moiety. The absorption spectra is almost independent on the solvent polarity. The fluorescence emission of the dyads were also studied. For **B-1**, the fluorescence is at 660 nm (in toluene. Fig. 1b). The emission band was red-shifted to 674 nm in dichloromethane (DCM). The emission profile is similar to the reference **B-5** (see ESI †, Fig. S58). The S_1 state energy of the Bodipy antenna is approximated as 1.88 eV with the emission wavelength, which is higher than the C_{60} moeity (1.76 eV).[23] Thus photoinduce RET is possible in **B-1**.

The emission band of **B-2** is at 770 nm in DCM. Thus the S_1 state energy of the Bodipy antenna in **B-2** can be approximated as 1.61 eV. The S_1 state energy level of the antenna in **B-2** is lower than the C_{60} moiety (1.76 eV),[23] as a result, the RET to C_{60} in **B-2** may be frustrated. The emission of **B-2** is more sensitive to the solvent polarity, thus more significant ICT is proposed for the antenna in **B-2**. The emission profile is similar to the reference compounds **B-6** (see ESI†, Fig. S59) The absorption and the fluorescence of the reference compounds **B-5** and **B-6** were also studied (see ESI†, Fig. S58-S59). The results are similar to that of **B-1** and **B-2**, respectively.

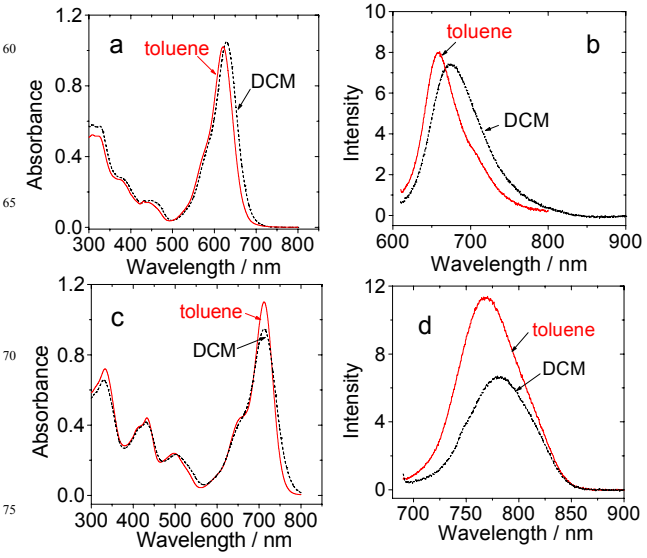

Fig. 1 (a) UV−Vis absorption spectra of **B-1** in toluene and DCM and (b) the corresponding emission spectra of **B-1**. λ_{ex} = 600 nm. A = 0.618, (c) UV−Vis absorption spectra of **B-2** in toluene and DCM and (d) the corresponding emission spectra of the **B-2**. λ_{ex} = 680 nm, A = 0.559. c = 1.0×10^{-5} M for UV−Vis absorption spectra measurement. 20 °C.

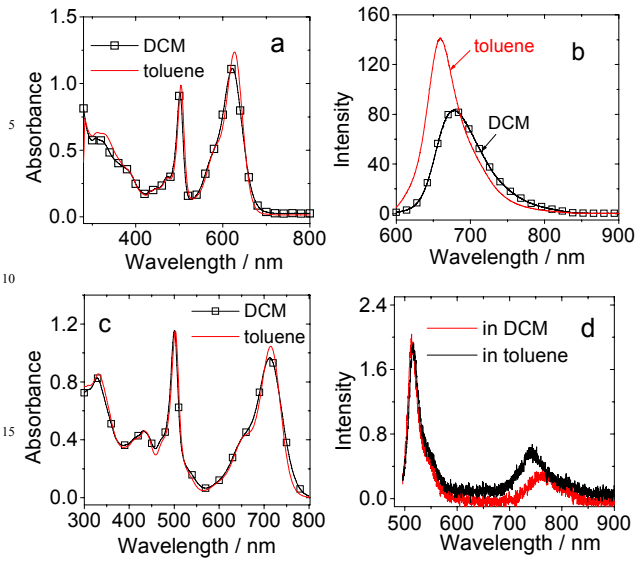

Fig. 2 (a) UV−Vis absorption spectra of **B-3** in DCM and toluene and (b) the corresponding emission spectra of **B-3**, λ_{ex} = 590 nm, A = 0.60, (c) UV−Vis absorption spectra of **B-4** and (d) the corresponding emission spectra of **B-4**, λ_{ex} = 486 nm, A = 0.51. c = 1.0 × 10^{-5} M for the UV−Vis absorption spectral measurement. 20 °C.

Two major absorption bands in visible spectral region were observed for triad **B-3** (Fig. 2a), which are attributed to the Bodipy and the dimethylaminostyryl Bodipy moiety in **B-3**, respectively. Emission of the Bodipy moiety was completely quenched in **B-3**, only an emission band at 675 nm was observed (Fig. 2b), which is due to the dimethylaminostyryl Bodipy moiety. This result indicated singlet EnT. This property was supported by the emission of the antenna **B-7** (see ESI†. Fig. S61). Broadband absorption was also observed for **B-4** (Fig. 2c). The emission of **B-4** is red-shifted as compared with that of **B-3**. For **B-4**, residual emission at 516 nm was observed.

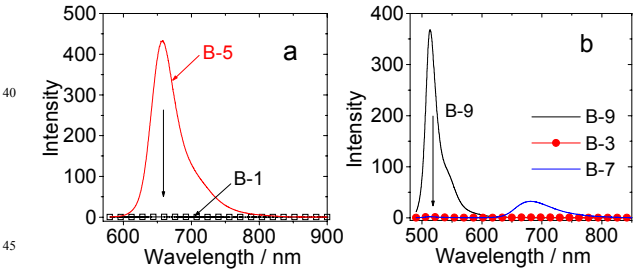

Fig. 3 Fluorescence of dyads **B-1** and triad **B-3** and the reference compounds. (a) Fluorescence emission spectra of **B-1** and **B-5**. λ_{ex} = 575 nm (A = 0.42 for both **B-1** and **B-5**). (b) Fluorescence emission spectra of **B-3**, **B-7** and **B-9**. λ_{ex} = 480 nm (A = 0.27 for **B-3**, **B-7** and **B-9**). c = ca. 1.0 × 10^{-5} M in DCM, 20 °C.

The fluorescence emission of **B-1** and the visible light-harvesting antenna **B-5** was compared (Fig. 3). The strong fluorescence of **B-5** (Φ_F = 47 %) was quenched in **B-1** (Φ_F = 0.1%). For **B-2**, similar results were observed (see ESI†, Fig. S70a). Similar results were observed for **B-3**, the reference compounds (Fig. 3b) and **B-4** (see ESI, Fig. S70b). These quenching of the fluorescence of the energy donor in the dyads or triads indicated EnT or ET, with the C_{60} as the energy or electron acceptor.[23,33] Similarly, the emission of **B-6** was substantially quenched in **B-2** (see ESI†, Fig. S70a). Same quenching effect was also found for **B-9** and **B-8** in **B-4** (see ESI†, Fig. S70).

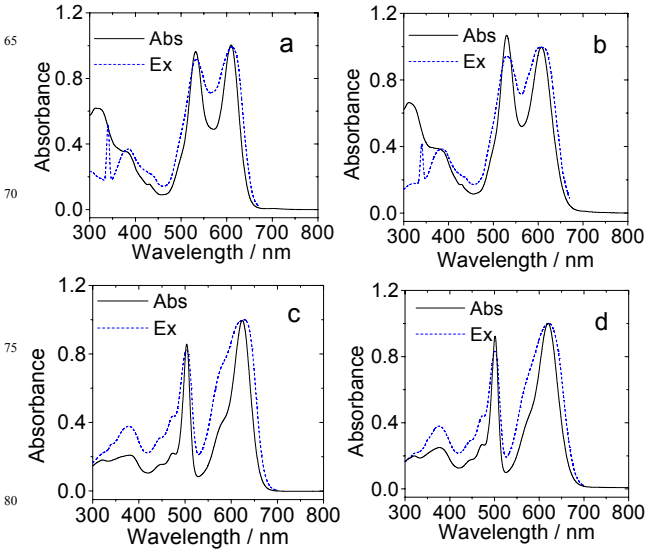

Fig. 4 Comparison of the fluorescence excitation spectra and UV−Vis absorption spectra of **B-3′** or **B-3** in different solvents. (a) **B-3′** in toluene; and (b) **B-3′** in DCM, λ_{em} = 680 nm; (c) **B-3** in toluene and (d) **B-3** in DCM, λ_{em} = 700 nm. c = 1.0 × 10^{-5} M, 20 °C.

The singlet state EnT in the compounds were studied with the fluorescence excitation spectra, examplified with triad **B-3** and **B-3′** (Fig. 4).[32] In toluene, the excitation spectrum of **B-3** (or **B-3′**) is superimposable with the UV−Vis spectrum (Fig. 4a and 4c). Thus the singlet EnT from the Bodipy moiety to the styryl-Bodipy moiety in **B-3** and **B-3′** is close to unity (95% and 96%). Moreover, the singlet EnT between the Bodipy and the styrylBodipy part takes place first, not the EnT between Bodipy and the C_{60} moiety, otherwise no excitation band at 531 nm should be observed for **B-3**. In polar solvent such as DCM, the comparison of the excitation spectrum with the UV−Vis absorption spectrum indicated that the energy transfer is slightly less efficient (85% and 88 %. Fig. 4b and 4d). This may be due to the more significant ET in polar solvents.[23] The emission of **B-4** is too weak to be used for excitation spectra study. Therefore the fluorescence excitation spectra of **B-8** were studied (see ESI†, Fig. S69). The singlet EnT efficiency is 75% in toluene, and 66% in DCM

Changes of the UV−Vis absorption and fluorescence spectra upon addition of acid

Protonation of the aminostyryl Bodipy in the dyads and the triads will change the absorption and fluorescence emission wavelength of the antennas.[6,28] Thus, the UV−Vis absorption spectra and the fluorescence spectra of the compounds were studied upon addition of trifluoroacetic acid (TFA. Fig. 5). For **B-1**, the absorption band at 623 nm decreased and a new absorption band at 573 nm developed upon addition of TFA. Accordingly, the emission band is blue-shifted from 674 nm to 591 nm upon addition of TFA (Fig. 5a and 5b). The changes can be better

studied with the antenna alone, i.e. **B-5** (see ESI†, Fig. S63) beacuse the fluorescence of **B-5** is much stronger than that of **B-1**.

For **B-2**, the absorption band at 712 nm decreased upon addition of TFA, and a new absorption band at 627 nm developed concomittantly (Fig. 5c), accordingly the fluorescence band shows blue-shifting from 770 nm to 644 nm (Fig. 5d). Based on

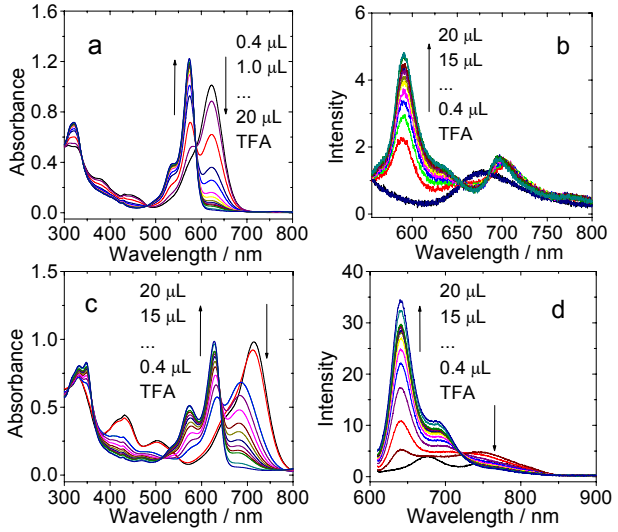

Fig. 5 Variation of the UV−Vis absorption spectra and the fluorescence emission spectra of **B-1** and **B-2** upon protonation with trifluoroacetic acid (TFA). (a) **B-1** with increasing TFA added and (b) the corresponding emission spectra of **B-1** (λ_{ex} = 540 nm) upon addition of TFA; (c) **B-2** with increasing TFA added and (d) the corresponding emission spectra changes of **B-2** (λ_{ex} = 600 nm) upon addition of TFA. The aliquots of TFA added are 0.4 μL, 1 μL, 2 μL, 3 μL, 4 μL, 5 μL, 10 μL, 20 μL and of 1 M TFA in CH_2Cl_2. c = 1.0 × 10^{-5} M in DCM, 20 °C.

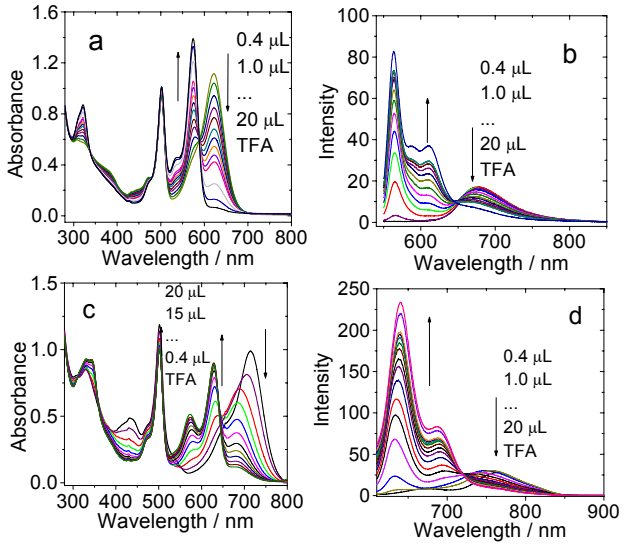

Fig. 6 Variation of the UV-Vis absorption spectra and the fluorescence emission spectra of **B-3** and **B-4** upon protonation with addition of TFA. (a) **B-3** with increasing TFA added and (b) the corresponding emission spectra changes of **B-3** (λ_{ex} = 540 nm) upon addition of the TFA. (c) **B-4** with increasing TFA added and (d) the corresponding emission spectra changes of **B-4** (λ_{ex} = 600 nm) upon addition of TFA. In CH_2Cl_2, (1.0 × 10^{-5} M; 20 °C). The aliquots of TFA added are 0.4μL, 1 μL, 2 μL, 3 μL, 4 μL, 5 μL, 10 μL, 20 μL of 1 M TFA in CH_2Cl_2 (c = 1.0 × 10^{-5} M in DCM, 20 °C).

these blue-shifting in the UV−Vis absorption and fluorescence emission spectra, we propose that the EnT from the styryl Bodipy part to the C_{60} moeity can be switched on by addition of TFA. The response of **B-6** to addition of TFA was studied, similar UV-Vis absorption and fluorescence emission spectral changes were observed (see ESI†, Fig. S63). Similar blue shifting were observed in the UV−Vis absorption and the fluorescence emission spectra of the triads **B-3** and **B-4** (Fig. 6). The response of **B-7** and **B-8** to addition of TFA was studied, similar UV−Vis absorption and fluorescence emission spectral changes were observed (see ESI†, Fig. S64).

Nanosecond time-resolved transient difference absorption spectra

In order to study the triplet excited state of the compounds, the nanosecond time-resolved transient difference absorption spectra of the compounds were studied (Fig. 7). The lifetime of the transient is usually the lifetime of the triplet state.[12] For **B-1**, bleaching band at 622 nm was observed upon pulse laser excitation in toluene (Fig. 7a), where the dimethylaminostyryl Bodipy shows strong steady state absorption. Thus the triplet excited state is localized on the styryl Bodipy moiety, not the C_{60} moiety. The triplet state lifetime was determined as 168.6 μs. Therefore, different from the direction of the singlet EnT, i.e. RET process, a reversed triplet EnT from the C_{60} moiety to the styryl Bodipy takes place. Such a ping-pong EnT was observed for C_{60}-chromophore hybrids.[29,34,35]

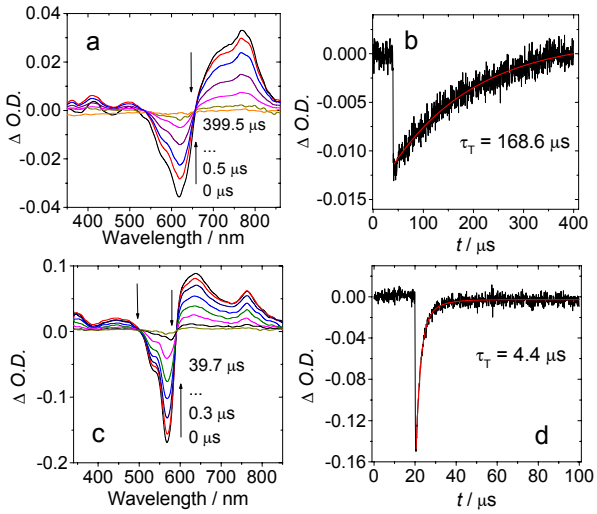

Fig. 7 Nanosecond time−resolved transient difference absorption of **B-1** in different solvents. (a) Transient absorption spectra and (b) decay trace at 580 nm in deaerated toluene; (c) Transient absorption spectra with 20 μL of 1 M TFA added and (d) the corresponding decay trace at 580 nm, in deaerated dichloromethane. Exited with nanosecond pulsed laser at λ_{ex} = 532 nm. c = 1.0 × 10^{-5} M, 20 °C.

In polar solvent, such as DCM, no transient signal was detected, which can be attributred to ET, which is usually more favored in polar solvent than that in non-polar solvent (see later electrochemical studies).[23] In the presence of TFA, bleaching band at 573 nm was observed (Fig. 7c), which is in agreement with the steady-state absorption spectra of **B-1** in acidic DCM (Fig. 7). The new triplet state is localized on the protonated

Table 1. Photophysical parameters of **B-1**–**B-8** with acid (trifluoroacetic acid, TFA) added [a]

	λ_{abs} (nm)	ε / 10^5 M^{-1} cm^{-1} [b]	λ_{em} (nm)[c]	Φ_L(%) [d]	τ_T (μs)[e]	τ_F (ns)[f]	ΔE_{st} [g]
B-1	573	1.20	591	0.3	4.4	–[h]	18
B-2	627	1.09	644	0.4	74.8	–[h]	17
B-3	504/574	0.96/1.33	587	1.8	4.3	–[h]	83/13
B-3′	522/559	1.12/1.20	573	0.7	121.8	–[h]	51/14
B-4	502/627	0.93/0.97	637	0.9	35.0	–[h]	135/10
B-5	569	1.13	592	37.2	–[h]	4.31	23
B-6	629	1.09	645	25.9	–[h]	3.89	16
B-7	502/574	1.01/1.05	592	62.7	–[h]	4.32	90/18
B-7′	527/559	1.19/1.45	572	36.5	–[h]	4.08	45/13
B-8	501/630	0.94/1.09	646	20.9	–[h]	4.63	145/16

[a] c = 1.0×10^{-5} M with 20 μL 1 M TFA added. at 20 °C [b] Molar extinction coefficient at the absorption maxima. [c] The emission maxima. [d] Fluorescence quantum yields with **B-12** (Φ_F = 9.5%, in toluene) as standard. [e] Triplet excited state lifetime. [f] Fluorescence lifetime. [g] Stokes shift. In nm. [h] Not observed.

Bodipy ligand, but the triplet excited state is different from that for **B-1** in toluene. Note the transient difference absorption profile in 600 – 850 nm is different for Fig. 7a and 7b. The triplet state lifetime was determined as 4.4 μs. The observation of TA signal in acidic DCM is due to the inhibited ET by the protonation, thus the inhibition of the ET process.

The nanosecond time-resolved transient difference absorption spectra of **B-2** were also studied (Fig. 8). No transient spectra was observed in toluene. Electron transfer is usually difficult to take place in non-polar solvents, such as toluene.[23] This result can be attributed to the lower S_1 state energy level of antenna (1.67 eV) than the S_1 state of C_{60} (1.76 eV),[23] i.e. there is no RET for **B-2** in toluene, as a result, no triplet state can be produced. In order to validify this conclusion, $^1O_2$ photosensitizing study was performed, no $^1O_2$ production was observed for for **B-2** in toluene (see ESI†, Fig. S78-79).

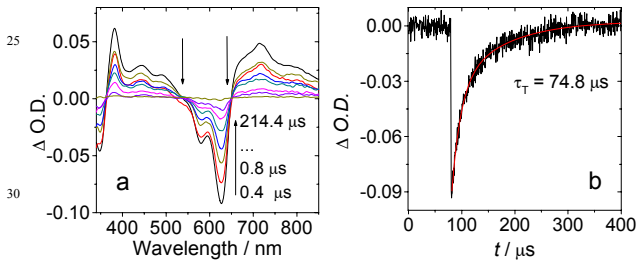

Fig. 8 Nanosecond time-resolved transient difference absorption spectra of **B-2**. (a) Transient absorption difference spectra and (b) the decay trace at 630 nm. In deaerated DCM with 20 μL of 1 M TFA added. λ_{ex} = 532 nm (c = 1.0×10^{-5} M, 20 °C).

In DCM, no transient spectra was observed. In DCM with TFA added, however, a bleaching band at 627 nm was observed (Fig. 8a), which is in agreement with the steady state absorption of the protonated **B-2**. Thus the triplet state is localized on the protonated Bodipy ligand. A triplet state lifetime of 74.8 μs was observed (Fig. 8b). Based on the nanosecond TA data, we propose the EnT in **B-2** was modulated by addition of acid, i.e. protonation of the aminostyryl Bodipy antenna. This is different from **B-1**, for which the ET was inhibited by addition of TFA.

Similar transient absorption spectra were observed for **B-3** (Fig. 9) as compared with that of **B-1**. Bleaching band at 625 nm was observed upon pulsed laser excitation in toluene. Positive transient absorption in the region of 670 – 850 nm region were observed. Exceptionally long triplet state lifetime of 333.7 μs was determined. These features are close to that of **B-1** under the same conditions. Therefore, the triplet state is localized on styryl Bodipy part, not on the C_{60} moiety in **B-3**. In DCM with TFA added, a bleaching band at blue-shifted position of 571 nm was observed for **B-3** (Fig. 9c), which is in agreement with the steady state absorption of the protonated amino styryl Bodipy antenna in **B-3** (Fig. 6a). Thus the triplet state is localized on the protonated amino styryl Bodipy moiety in **B-3**. In this case a 'ping-pong' singlet/triplet energy transfer takes place.[28]

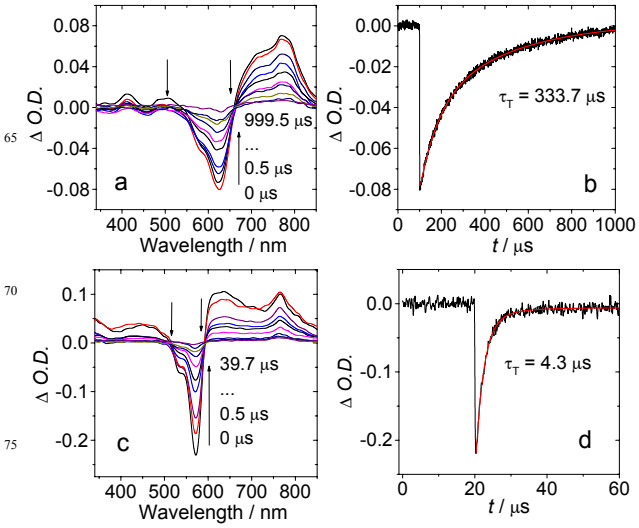

Fig. 9 Nanosecond time–resolved transient difference absorption of **B-3** in different solvents. (a) Transient difference absorption spectra and (b) decay trace at 620 nm in deaerated toluene; (c) Transient absorption difference spectra of **B-3** with 20 μL of 1 M TFA added and (d) the corresponding decay trace at 580 nm, in deaerated DCM. λ_{ex} = 532 nm, (c = 1.0×10^{-5} M, 20 °C)

Transient absorption spectra were observed for **B-3′** (Fig. 10) as compared with that of **B-1** and **B-3**. Bleaching band at 600 nm was observed upon pulsed laser excitation in toluene. Positive transient absorption in the region of 650 – 850 nm region were observed (Fig. 10a). A triplet state lifetime of 140.1 μs was determined (Fig. 10b). These features are close to that of **B-1** under the same conditions. Therefore, the triplet state is localized

on the styryl Bodipy part, not on the Bodipy moiety or C_{60} moiety in **B-3′**.

Different from **B-1** and **B-3**, transient absorption spectra were observed for **B-3′** in DCM (Fig. 10c). The feature of the transient spectra are similar to that in toluene. A triplet state lifetime of 100.7 μs was observed (Fig. 10d). The slightly decreased triplet state lifetime in DCM than that in toluene may be due the enhanced ET.[23] However, we propose that photo-induced ET is not significant, otherwise the triplet state will be quenched, like in **B-1** and **B-3**. The thermodynamic driving force for photoinduced

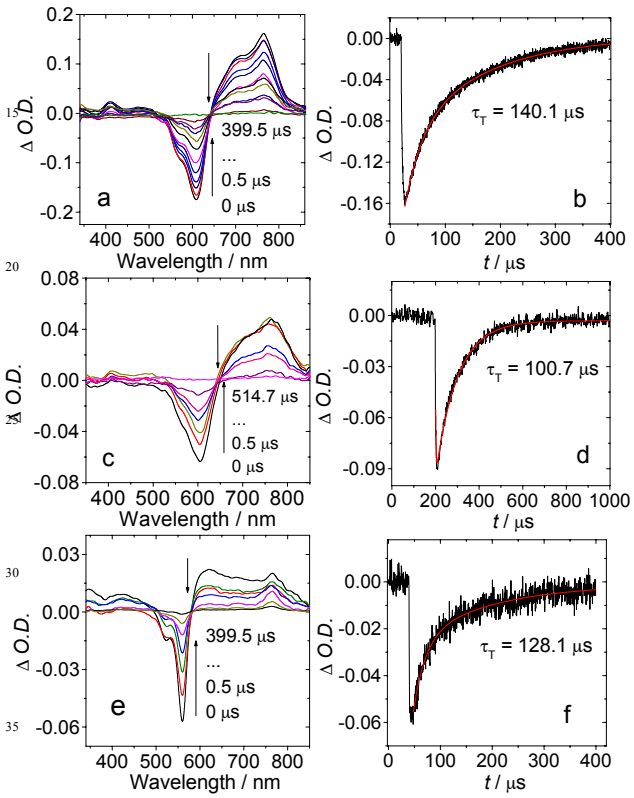

Fig. 10 Nanosecond time-resolved transient difference absorption spectra of **B-3′** in different solvents. (a) Transient spectra and (b) the corresponding decay trace at 620 nm. In deaerated toluene. (c) Transient spectra in deaerated dichloromethane and (d) the corresponding decay trace at 620 nm; (e) Transient spectra of **B-3′** in deaerated DCM with 20 μL of 1 M TFA added and (f) the corresponding decay trace at 570 nm. λ_{ex} = 532 nm, $c = 1.0 \times 10^{-5}$ M, 20 °C.

electron transfer was calculated with the Weller equation. **B-3** is with slightly larger driving force (ΔG^{o}_{cs} = −0.68 eV) than **B-3′** (ΔG^{o}_{cs} = −0.65 eV). The charge transfer state energy level (E_{CTS} = 1.26 eV) is higher than triplet state energy level (T_1 = 1.24 eV by DFT calculated. In DCM). But for **B-1**, the charge transfer state energy level (E_{CTS} = 1.14 eV) is lower than triplet state energy level, thus it is effective for quenching the triplet state though electron transfer. In toluene, the Gibbs free energy was calculated for **B-3** (ΔG^{o}_{cs} = −0.18 eV) and **B-3′** (ΔG^{o}_{cs} = +0.17 eV). From the above analysis, it can be deduced that the electron transfer of **B-3** is more significant than **B-3′**.

In DCM with TFA added, a bleaching band at blue-shifted position of 557 nm was observed for **B-3′** (Fig. 10e), which is in agreement with the steady state absorption of the protonated amino styryl Bodipy antenna in **B-3′**. Thus the triplet state is localized on the protonated amino styryl Bodipy moiety in **B-3′**, not on the Bodipy or the C_{60} moiety. In this case a 'ping-pong' singlet/triplet EnT takes place.[28] Note the triplet state lifetime is different from the neutral **B-3**'.The transient spectra of **B-3′** indicated that the ET is less significant as compared to that of **B-1** and **B-3**. We attributed this difference in ET capability to the different structure of the antenna. In **B-3′**, the distance between the electron donor and C_{60} moiety (electron acceptor) is larger than that in **B-1**.

For **B-4**, no transient signal can be detected and no $^1O_2$ produced in both toluene and DCM (Fig. S78-79). It is most likely due to the unmathced S_1 state of the antenna and the C_{60} moiety. In DCM with TFA added, bleaching band at 627 nm was detected (Fig. S83a). Thus the triplet excited state is localized on the aminostyryl Bodipy antenna, not on the C_{60} moiety. The production of triplet excited state in the presence of TFA is due to the increased energy level of the S_1 state of the antenna, thus the acid-activated EnT to C_{60} occured. The results of the triads **B-3** and **B-4** indicated that the RET from Bodipy to C_{60} is not taking place, rather the sequential Bodipy→aminostyryl Bodipy→C_{60} process is taking place in the triads.

Electrochemical studies

The electrochemical property of **B-1** and reference **B-5** was studied in DCM (Fig. 11 and Table 2. for **B-3**, **B-4** and reference compounds, see ESI†, Fig. S71-S74 and Table 2). For **B-5**, there are two reversible oxidation waves at +0.34 V, +0.66 V, and one reversible reduction wave at −1.41 V. For **B-1**, in the anodic scan, two reversible oxidiation waves at around +0.35 V, +0.67 V were observed. In the cathodic scan, two reversible reduction potential was observed for **B-1** (−0.97eV, −1.38 eV), which are dur to fullerene. In order to study electron transfer from dimethylaminostyryl Bodipy to fullerene, the Gibbs free energy (ΔG^{o}_{cs}) was calculated. From the ΔG^{o}_{cs} analysis, some results have been found, In polar solvent, the free energy changes of **B-1** in CH_2Cl_2 (ΔG^{o}_{cs} = −0.74 eV) is larger than that in nopolar solvent (ΔG^{o}_{cs} = −0.24 eV in toluene). Therefore the triplet state is unlikely to be observed in the polar solvent. For **B-2**, the free energy changes is large in DCM (ΔG^{o}_{cs} = −0.74 eV), thus the fluorescence emission is effectively quenched by photoinduced intramolecular electron transfer (Fig. 1). In nopolar solvent toluene, the S_1 energy level is 1.67 eV for dimethylaminodistyryl Bodipy lower than C_{60} (1.76 eV), therefore no triplet state

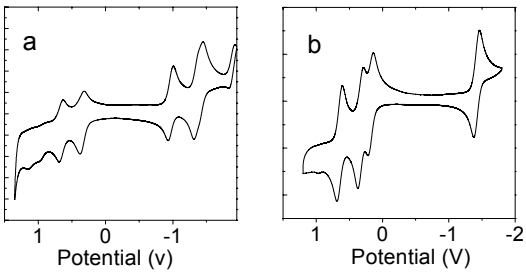

Fig. 11 Cyclic voltammogram of **B-1** and **B-5**. (a) **B-1**, (b) **B-5**. Ferrocene (Fc) was used as internal reference ($E_{1/2}$ = +0.64 V (Fc^+/Fc) vs. standard hydrogen electrode). In deaerated CH_2Cl_2 solutions and 0.10 M Bu_4NPF_6 as supporting electrode, Ag/$AgNO_3$ reference electrode, Scan rates: 100 mV/s. 20 °C.

Table 2. Redox potentials of Bodipy-C_{60} photosensitizers. Anodic and cathodic wave potentials were presented vs. saturated calomel electrode [a]

	E(ox) (V)	*E*(red) (V)
B-1	+0.35, +0.67	−0.97, −1.38, −1.88
B-2	+0.14, +0.28, +1.01	−0.97, −1.36
B-3	+0.42, +0.74, +1.03	−0.96, −1.12, −1.49, −1.89
B-3′	+0.36, +0.63, +0.97	−0.96, −1.39, −1.87
B-4	+0.15, +0.91, +1.09	−0.92, −1.32, −1.47, −1.86
B-5	+0.34, +0.66	−1.41
B-6	+0.25, +1.02	−1.35
B-7	+0.35, +0.73, +1.02	−1.32, −1.43
B-7′	+0.37, +0.64, +0.93	−1.42
B-8	+0.17, +0.93, +1.06	−1.32, −1.46

[a] Cyclic voltammetry in N_2 saturated CH_2Cl_2 containing a 0.10 M Bu_4NPF_6 supporting electrolyte; Counter electrode is Pt electrode; working electrode is glassy carbon electrode; $Ag/AgNO_3$ couple as the reference electrode. *c* [Ag^+] = 0.1 M. 20 °C. Conditions: 0.5 mM photosensitizers in CH_2Cl_2, 298 K.

was observed for **B-2** because RET can not occur. Similar results were observed for **B-3** and **B-4** (Table 2, 3 and Fig. S71-S74). These electrochemical data can be used for explain the triplet state properties of the dyads/triads in solvent with different polarity. For example, the free energy changes for ET in polar solvent is usually large than that in nonpolar solvent such toluene. This is true for **B-1** and **B-2**, etc. Upon protonation, the ET process was prohibited, thus triplet state can be observed for the dyads/triads.

Application of the acid-activated triplet state production: singlet oxygen ($^1O_2$) photosensitizing

With the nanosecond time-resolved transient difference absorption spectroscopy, we demonstrated that the production of the triplet excited state by the dyads and the triads can be switched by acid. Therefore, the switching of the $^1O_2$ photosensitizing ability of the dyads and the triads were studied (Fig. 12).[12] 1,3-diphenylisobenzofuran (DBPF) was used as the $^1O_2$ scavenger. Thus the absorption of DBPF at 414 nm can be followed to monitor the kinetics of the $^1O_2$ production of the dyads and the triads upon visible light photoirradiation.[36,37]

For **B-1**, no $^1O_2$ production can be observed in the absence of acid (TFA) (Fig. 12a). In the presence of acid (TFA, Fig. 12b), the absorbance of the solution at 414 nm decrease sharply upon photoexcitation, indicating that $^1O_2$ was produced in a signifcant fast kineics, i.e. the triplet state production of **B-1** is switched ON. Note DPBF alone is stable under the same condition (see ESI†, Fig. S95), thus the $^1O_2$ photosensitizing was confirmed.

Similar studies were applied for **B-3** and **B-4** (see ESI†, Fig. S94). No $^1O_2$ was produced in DCM upon photoexcitation. In the presence of TFA, photosensitization $^1O_2$ was observed. This observation is in agreement with the nanosecond time-resolved transient absorption spectra of **B-3** and **B-4**. Interestingly, no modulation on the $^1O_2$ photosensitizing of **B-3′** by addition of acid was observed. This phenomena is in agreement with the nanosecond time-resolved transient difference absorption spectra of **B-3′**, i.e. triplet state production was observed for **B-3′** in DCM, as well as in DCM with TFA added (see ESI†, Fig. S94). Thus the $^1O_2$ production of the triplet photosensitizers can be directly correlated to the triplet state production of the dyads and triads. $^1O_2$ photosensitizing of **B-4** can be switched by addition

Table 3. The thermodynamic driving force for photoinduced electron transfer was calculated from the Weller equation

	ΔG^o_{CS} (eV)[a]	ΔG^o_{CS} (eV)[b]	E_{CTS}/ eV[c]	E_{CTS}/ eV[d]
B-1	−0.74[e]/−0.10[f]	−0.24[e]/+0.40[f]	1.64	1.14
B-2	−0.74[e]/−0.19[f]	−0.24[e]/+0.31[f]	1.43	0.95
B-3	−0.68[e]/−0.04[f]	−0.18[e]/+0.46[f]	1.70	1.20
B-3′	−0.65[e]/+0.018[f]	+0.17[e]/+0.84[f]	2.08	1.26
B-4	−0.77[e]/−0.23[f]	−0.27[e]/+0.27[f]	1.39	0.89
B-7	−0.39[e]/+0.25[f]	+0.11[e]/+0.75[f]	–[g]	–[g]
B-7′	−0.18[e]/+0.49[f]	+0.64[e]/+1.31[f]	–[g]	–[g]
B-8	−0.34[e]/+0.19[f]	+0.16[e]/+0.69[f]	–[g]	–[g]

[a] In DCM. [b] In toluene. [c] $E_{CTS} = E_{1/2}(D^{\bullet+}/D) - E_{1/2}(A^{\bullet-}/A) + \Delta G_S$ where $E_{1/2}(D^{\bullet+}/D)$ is the first oxidation potential of the donor, $E_{1/2}(A/A^{\bullet-})$ is the first reduction potential of the acceptor, ΔG_S is he static Coulombic energy, the energy level of charge transfer state in toluene. [d] The energy level of charge transfer state in DCM. [e] ΔG^o_{CS} was calculated by Weller equation, photoinduced electron transfer from the S_1 state of styryl-Bodipy. [f] Photoinduced electron transfer from the T_1 state of styryl-Bodipy. [g] Not applicable.

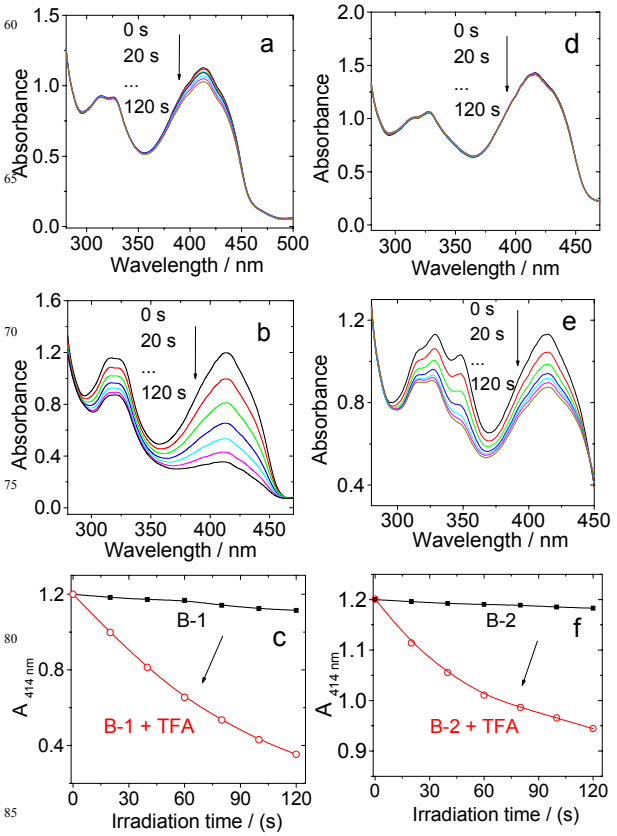

Fig. 12 Switching of the singlet oxygen ($^1O_2$) photosensitizing ability of **B-1** and **B-2** in the absence and the presence of TFA. The decreasing of the absorption of $^1O_2$ scavenger 1,3-diphenylisobenzofuran (DPBF) at 414 nm was monitored upon the monochromic light irradiation. UV–Vis absorption spectral changes **B-1** as photosensitizer (a) in the absence of TFA acid and (b) in the presence of TFA. (c) Absorbance of DPBF at 414 nm changes in the absence and in the presence of TFA (λ_{ex} =588 nm). UV/vis absorption spectral changes with **B-2** as photosensitizer, (d) in the absence of TFA and (e) in the presence of acid, (f) in absorbance of DPBF at 414 nm changes in the absence and in the presence of TFA (λ_{ex} = 646 nm). *c* [photosensitizers] = 1.0×10^{-5} M in CH_2Cl_2, 20 °C.

of acid (see ESI, Fig. S94), which is in agreement with the study of the triplet state production of **B-4** by the nanosecond time-resolved transient difference absorption spectra. More significant is that switching of the triplet state of photosensitizers is reversible by adding acid and base alternatively. When the acid was neutralized with base, the photophyscial properties of the photosentiziers fully recovered (see ESI†, Fig. S83-93).

The $^1O_2$ quantum yields (Φ_Δ) of the dyads and triads were measured in the absence and presence of TFA. For **B-1**, the Φ_Δ value is 1.9% in the absence of TFA. In the presence of TFA, Φ_Δ increased to 73% (Table 4). Similar switching effect was observe for **B-2**–**4**. For **B-3′**, however, the Φ_Δ value in the absence and in the presence of TFA is 30% and 39%, thus no switching effect of the triplet excited state production was observed for **B-3′**. This finding is in agreement with the nanosecond time-resolved transient difference absorption spectral studies of the compounds (Fig. 9).

Table 4. Singlet oxygen quantum yield (Φ_Δ) and triplet state lifetime (τ_T)

	τ_T (μs)	Φ_Δ [c]
B-1	168.6 [a]	1.9 %
B-2	– [a]	1.1 %
B-3	333.7 [a]	2.0 % / 1.8 %
B-3′	140.1 [a] / 100.7 [b]	30 % / 30 %
B-4	– [a]	1.0% / 1.4 %
	In the presence of TFA	
B-1	4.4 [b]	73 %
B-2	74.8 [b]	26 %
B-3	4.3 [b]	52 % / 63 %
B-3′	121.8 [b]	39 % / 53 %
B-4	35.0 [b]	22 % / 17 %

[a] Triplet lifetime in deaerated toluene. [b] Triplet lifetime in deaerated DCM. [c] Quantum yield of singlet oxygen ($^1O_2$). For short wavelength excitation, diiodoBodipy was used as standard (Φ_Δ = 0.82 in CH_2Cl_2), for the long wavelength excitation, methylene blue was used as standard (Φ_Δ = 0.57 in CH_2Cl_2).

Jablonski diagrams: Photophyical processes of the dyads/triads

The photophysical processes of **B-1** were summarized in Scheme 4. Upon selective photoexcitation into the styrylBodipy antenna in **B-1** (Scheme 4a), the singlet excited state of the antenna was produced firstly. Then via intramolecular energy transfer, the singlet excite state of the C_{60} moiety was produced. Then via the inherent ISC of C_{60}, the triplet state of C_{60} moiety was produced. Since the triplet state energy level of the styryl Bodipy is lower than that of C_{60} moiety, the intramolecular triplet state energy transfer is envisaged.

The charge transfer state (CTS) is with lower energy level than that of the T_1 state of styrylBodipy, thus the triplet state can be quenched by production of the CTS. In toluene, however, the CTS is with energy level of 1.64 eV, which is higher than that of the triplet state energy level of the styrylBodipy moiety. Thus the triplet state of the styrylBodipy will not be quenched by any CST. These postulations are in full agreement with the experimental results (Fig. 7). It should be pointed out the triplet state can be produced from the charge recombination process.[23,38]

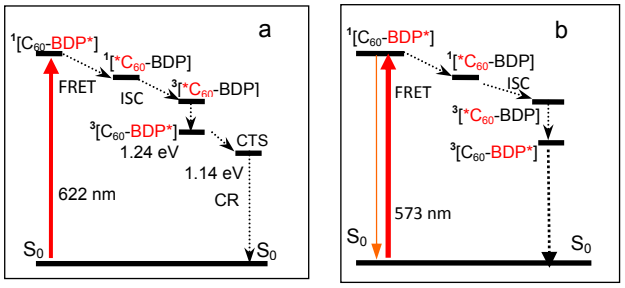

Scheme 4. Simplified Jablonski diagram illustrating the photophysical processes of **B-1** (a) in the absence and (b) in the presence of acid. CH_2Cl_2 was used as solvent. [C_{60}-BDP] stands for **B-1**. The localization of the excited state in the dyad was designated with red color and a asterisk. The number of the superscript designated spin multiplicity.

In the presence of **B-1** (Scheme 4b), the dimethylamino group is protonated, thus the CTS energy level will be promoted (data are unavailable due to the inteference of H^+ in the measurement of cyclic voltammetry). Thus, the triplet state of the protonated dimethylamino styrylBodipy moiety will not be quenched by CTS. Thus triplet state was detected for **B-1** even in polar solvents such as dichloromethane (Fig. 7).

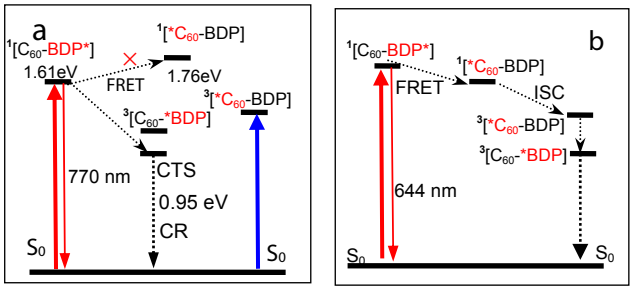

Scheme 5. Simplified Jablonski diagram illustrating the photophysical processes involved **B-2** (a) in the absence of acid and (b) in the presence of acid. [C_{60}-BDP] stands for **B-2**. The localization of the triplet state in the dyad was designated with red color and a asterisk. The number of the superscript designated the spin multiplicity of the excited state.

The photophysics of **B-2** is slightly different from that of **B-1** (Scheme 5). First, the S_1 state energy level of the dimethylaminostyrylBodipy part is lower than that of C_{60}, thus FRET is impossible (Scheme 5a). Second, CTS is with energy level of 0.95 eV, thus any triplet state localized on either the C_{60} or the dimethylaminostyrylBodipy will be quenched. This postulation is in agreement with the experimental results that no triplet excited state was observed for **B-2**, either in toluene or in dichloromethane, which is different from that of **B-1**.

In the presence of acid, such as TFA, the dimethylamino group is protonated, thus the S_1 state energy level becomes higher than the S_1 state of the C_{60} moiety, as a result the FRET is possible (Scheme 5b). Moreover, upon protonation, the CTS energy level is elavated (eaxct data are unknown due to the difficulty to record the electrochemical data of the protonated species). Thus triplet state was observed for **B-2** in the presence of TFA (Fig. 8).

Conclusions

In conclusion, in order to switch the triplet excited states of organic compounds, dimethylaminostyryl Bodipy-C_{60} dyads and triads were prepared. The designing rationales of these compounds are that either the photoinduced electron transfer (ET) or the singlet state energy transfer (EnT) from the visible light-harvesting antenna to C_{60} moiety can be switched by acid (protonation of the amino styryl moeity). C_{60} moiety in the dyads/triads is the electron or singlet energy acceptor, and the spin converter. Bodipy units ar the visible light harvesting antenna, the singet energy and electron donor. The triplet state of the compounds was studied in detail with nanosecond time-resolved transient difference absorption spectroscopy. For the dyad with the mono(4′-dimethylaminostyryl) Bodipy antenna, the triplet excited state was quenched by intramolduclar EnT in polar solvent. In presence of acid (trifluoroacetic acid), the dimethylaminostyryl Bodipy moiety is protonated, as a result, the ET was inhibited. Therefore the sequenctial EnT and the intersystem crossing of C_{60} process produce triplet excited state. For the dyad and the triads with bis(4-dimethylaminostyryl) substituted Bodipy antenna, the lower antenna S_1 state energy level than that of C_{60} prohibits any RET to C_{60}, thus no triplet state was produced. In the presence of acid thus protontation of the aminostyryl substituents, the UV−Vis absorption and the fluorescence emission show drastic blue shifting, and the S_1 state energy level of the antenna is increased to be higher than S_1 state of C_{60} moiety, as a result EnT is activated and triplet state will be produced. In all the compounds the triplet excited state is localized on the dimethylaminostyryl Bodipy moiety, not on the C_{60} moiety. We proved that the $^1O_2$ photosensitizing ability of the compounds can be switched by acid (the variation of the singlet oxygen quantum yield can be up to 30-fold). These studies will be useful for development of external stimuli-activatable triplet state production with organic chrmophores and for the application of these compounds in activatable photodynamic theraputic reagents, molecular devices and fundamental photochemistry studies.

Experimental section

General Methods. UV−Vis absorption spectra were taken on a HP8453 UV−Vis absorption spectrophotometer. Fluorescence spectra were recorded on a Shimadzu RF 5301PC spectrofluorometer. Luminescence lifetimes were measured on a OB 920 fluorescence/phosphorescence lifetime spectrometer. For the preparation of the intermediate compounds, please refer to the ESI †.

Compound B-1. Under Ar atmosphere, a mixture of compound **4** (28.0 mg, 0.05 mmol), fullerene (43.2 mg, 0.006 mmoL) and sarcosine (17.8 mg ,0.20 mmoL) were dissolved in dry toluene (50 mL). The mixture was refluxed for 12 h. After completion of the reaction, the mixture was cooled to room temperature (RT), After removal of the solvent under reduced pressure, the mixture was purified by column chromatography (silica gel, DCM) to give black solid. MP >250°C Yield: 40.5 mg (62 %). ^{1}H NMR (400 MHz, $CDCl_3$): δ = 7.84 (s, 2H), 7.54–7.50 (m, 3H), 7.47–7.45 (m, 3H), 7.33–7.31 (m, 2H), 7.24–7.20 (m, 3 H), 6.83 (s, 2 H), 6.62 (s, 1 H), 5.01 (s, 2H), 4.31 (s, 1H), 3.05 (s, 6H), 2.89 (s, 3H), 2.51 (s, 3 H), 1.57 (s, 3H), 1.42 (s, 3 H) ppm. ^{13}C NMR (100 MHz, $CDCl_3$): 147.3, 146.8, 146.7, 146.5146.4, 146.3, 146.2, 146.1, 146.0, 145.9, 145.8, 145.7, 145.5, 145.5, 145.4, 145.3, 1345.2, 145.1, 145.0, 144.9, 144.7, 144.4, 143.1, 143.0, 142.7, 142.6, 142.5, 142.4, 142.3, 142.1, 142.0, 141.9, 141.8, 141.7, 141.6, 141.5, 141.4, 140.5, 140.2, 140.1, 139.8, 139.7 139.5, 139.4, 139.2, 135.8, 135.7, 135.4, 134.4, 133.4, 129.3, 129.1, 128.9, 128.4, 117.9, 82.3, 40.1, 32.8, 31.9, 29.7, 14.7, 13.4, 12.7 ppm. HRMS (MALDI): *m*/*z* calcd for $[C_{97}H_{37}BF_2N_4]^-$: 1306.3079; found 1306.3124.

Compound B-2. The compound was prepared with the same methods of **B-1**. **B-2** was purified by chromatography (silica gel, DCM) to give black solid. Yield: 28.8 mg (57 %). MP > 250°C . ^{1}H NMR (400 MHz, $CDCl_3$): δ = 7.97–7.77 (m, 5H), 7,52–7.44 (m, 5H), 7.35–7.32 (m, 5H), 7.11–7.10 (m, 2H), 6.63–6.53 (m, 5H), 5.04–4.96 (m, 2H), 4.28–4.26 (m, 1H), 2.80 (s, 3H), 1.54 (s, 3H), 1.43 ppm (s, 3H). ^{13}C NMR (100 MHz, $CDCl_3$): 156.3, 154.1, 153.6, 153.4, 147.4, 147.3, 146.7, 146.5, 146.3, 146.2, 146.1, 146.0, 145.8, 145.6, 145.5, 145.4, 145.3, 145.2, 145.1, 144.8, 144.5, 144.4, 144.3, 143.1, 143.0, 142.7, 142.6, 142.5, 142.3, 142.2, 142.1, 142.0, 141.9, 141.8, 141.7, 141.6, 141.5, 141.4, 141.3, 141.2, 140.2, 139.9, 139.5, 137.0, 136.6, 135.9, 135.8, 129.5, 128.9, 128.7, 112.5, 112.3, 112.2, 112.1, 83.6, 70.0, 69.1, 68.1, 40.0, 25.6, 14.7, 12.4 ppm. HRMS (MALDI): *m*/*z* calcd for $[C_{106}H_{46}BF_2N_5]^-$: 1437.3814; found 1437.3922.

Compound B-3. The preparation procedure is similar to that of **B-1**. **B-3** was purified by chromatography (silica gel, DCM) to give black solid. Yield: (26.0 mg, 49 %). MP >250°C. ^{1}H NMR (400 MHz, $CDCl_3$): δ = 7.90 (s, 1H), 7.75 (s, 1H), 7.53–7.50 (m, 3 H), 7.24–7.17 (m, 8H), 7.11 (d, 2H, *J* = 8.4 Hz), 6.98 (d, 2H, *J* = 8.0 Hz), 6.79 (s, 2H), 6.61 (s, 1H), 5.98 (s, 2H), 5.25 (s, 2H), 5.03 (s, 2H), 4.83–4.82 (m, 2H), 4.44–4.42 (m, 2H), 4.31 (s, 1H), 3.05 (s, 6H), 2.88 (s, 3H), 2.56 (s, 6H), 2.51 (s, 3H), 1.44 (s, 3H), 1.42 (s, 6H), 1.27 ppm (s, 3H). ^{13}C NMR (100 MHz, $CDCl_3$): 158.86, 158.24, 155.39, 147.32, 147.29, 146.69, 146.44, 146.29, 146.26, 146.22, 146.17, 146.11, 146.09, 145.93, 145.92, 145.74, 145.56, 145.53, 145.44, 145.36, 145.27, 145.22, 145.17, 145.15, 144.70, 144.52, 144.39, 144.32, 143.75, 143.13, 143.07, 142.98, 142.87, 142.59, 142.56, 142.53, 142.23, 142.17, 142.05, 141.90, 141.89, 141.76, 141.68, 141.52, 141.48, 140.18, 140.13, 139.78, 139.60, 136.16, 135.89, 135.75, 133.74, 131.80, 131.11, 130.43, 129.96, 129.36, 128.79, 127.75, 124.13, 121.25, 118.01, 225.36, 115.00, 83.24, 66.33, 61.99, 49.88, 39.99, 31.93, 29.69, 15.05, 14.63, 14.13, 13.38, 12.97. HRMS (MALDI): *m*/*z* calcd for $[C_{121}H_{61}B_2F_4N_9O_2]^+$: 1769.5070; found 1769.4987.

Compound B-4. The preparation procedure is similar to that of **B-1**. **B-4** was purified by chromatography (silica gel, DCM) to give black solid. Yield: 23.9 mg (38 %). MP >250°C. ^{1}H NMR (400 MHz, $CDCl_3$): δ = 7.90 (s, 2H), 7.68–7.52 (m, 5H), 7.33–7.31 (m, 3H), 7.22–7.18 (m, 5H), 7.12–7.09 (m, 4H), 6.99–6.95 (m, 4H), 6.80–6.69 (m, 5H), 5.98 (s, 2 H), 5.25 (s, 2 H), 5.00 (s, 2H), 4.83–4.80 (m, 2H),4.43–4.40 (m, 2H), 4.28 (s, 1 H), 3.05 (s, 12H), 2.17 (s, 3 H), 2.08 (s, 6H), 1.59 (s, 6H), 1.42 (s, 6H). ^{13}C NMR (100 MHz, $CDCl_3$): δ = 158.83, 158.25, 155.40, 147.37, 147.30, 147.27, 146.37, 146.29, 146.24, 146.23, 146.15, 146.12, 146.04, 145.98, 145.95, 145.79, 145.59, 145.53, 145.49, 145.40, 145.36, 145.34, 145.23, 145.18, 145.10, 144.96, 144.92,

144.88, 144.82, 144.77, 144.75, 144.72, 144.54, 144.42, 144.37, 144.35, 144.29, 144.26, 143.75, 143.14, 143.10, 143.07, 143.01, 142.73, 142.65, 142.63, 142.60, 142.55, 142.23, 142.11, 142.07, 141.96, 141.90, 141.75, 141.73. 141.51, 141.44, 140.22, 139.86, 139.35, 135.95, 135.69, 131.76, 129.36, 127.76, 124.15, 121.24, 115.37, 115.01, 66.35, 65.84, 62.01, 49.88, 39.94, 30.94, 29.72, 15.28, 15.02, 14.63, 12.72. HRMS (MALDI): *m/z* calcd for $[C_{130}H_{70}B_2F_4N_{10}O_2]^+$: 1900.5805; found 1900.5927, $[M\text{-}F]^+$1880.6173, $[M\text{-}C_{60}]^+$1181.6094.

Compound B-5. Under Ar, a mixture of **2** (58.1 mg, 0.1 mmol), phenylboronic acid (72 mg, 0.6 mmoL) and K_2CO_3 (41.7 mg , 0.3 mmoL) was dissolved in toluene/ethanol/water (15 mL, 2/2/1, v/v), and the mixture was bubbled with Ar for 15 min. $Pd(PPh_3)_4$ (18.1 mg, 0.015 mmoL) was added. The mixture was refluxed for 3 h. After completion of the reaction, the mixture was cooled to RT, water (30 mL) was added, and the mixture was extracted with dichloromethane (3×50 mL). The organic layers were dried over Na_2SO_4. After removal of the solvent under reduced pressure, the mixture was purified by column chromatography (silica gel, DCM/petroleum = 1:1, v/v) to give deep purple solid. Yield: 47.8 mg (90 %). ^{1}H NMR (400 MHz, $CDCl_3$): δ = 7.55 (d, 3H, *J* = 8.4 Hz), 7.48 (d, 3H, *J* = 6.4 Hz), 7.30 (d, 1H, *J* = 8.0 Hz), 7.23 (d, 1H, *J* = 16.0 Hz), 7.16 (d, 2H, *J* = 7.6 Hz), 6.99 (s, 2H), 6.61 (s, 1H), 3.05 (s, 6H), 2.55 (s, 3H), 1.42 (s, 3H), 1.29 ppm (s, 3H). ^{13}C NMR (100 MHz, $CDCl_3$): 154.9, 151.7, 143.0, 139.3, 137.8, 135.7, 134.3, 133.5, 133.1, 131.0, 130.6, 130.4, 129.9, 129.4, 129.2, 129.0, 128.6, 128.4, 126.2, 118.0, 114.9, 112.5, 40.7, 29.9, 14.9, 12.7 ppm. HRMS (MALDI): *m/z* calcd for $[C_{34}H_{32}BF_2N_3]^+$: 531.2657; found 531.2694.

Compound 10. Under Ar, a mixture of **8** (41.0 mg, 0.10 mmol), **7** (66.7 mg, 0.10 mmoL) were dissolved in $CHCl_3$/EtOH/H_2O (14 mL, 12/1/1, v/v), $CuSO_4{\cdot}5H_2O$ (2.5 mg, 0.10 mmoL) and sodium ascorbate (3.8 mg, 0.020 mmoL) were added. The mixture was stired at RT for 24 h. After completion of the reaction, the mixture was washed in water (3×20 mL). The organic layers were dried over Na_2SO_4. After removal of the solvent under reduced pressure, the mixture was purified by column chromatography (silica gel, DCM/methanol = 100/1, v/v) to give black solid. Yield: 93.9 mg (90 %). ^{1}H NMR (400 MHz, $CDCl_3$): δ = 7.92 (s, 1 H), 7.52–7.45 (m, 3H), 7.28 (s, 1H), 7.24 (s, 1H), 7.21–7.17 (m, 4H), 7.13 (d, 2H, *J* = 8.4 Hz), 7.00 (d, 2H, *J* = 8.0 Hz), 6.72 (d, 2H, *J* = 5.2 Hz), 6.64 (s, 1H), 5.97 (s, 2H), 5.27 (s, 2H), 4.85–4.83 (m, 2H), 4.47–4.44 (m, 2H), 3.04 (s, 6H), 2.65 (s, 3H), 2.55 (s, 6H), 1.42 (s, 9H), 1.40 ppm (s, 3H). HRMS (MALDI): *m/z* calcd for $[C_{52}H_{51}B_2F_4N_8O_2I]^+$: 1044.3302; found 1044.3279.

Nanosecond time-resolved transient difference absorption spectroscopy

Nanosecond time-resolved transient difference absorption spectra were recorded on a LP 920 laser flash photolysis spectrometer (Edinburgh Instruments, Livingston,UK). The sample solutions were purged with N_2 for 20 min before measurements were taken. The samples were excited with 532 nm nanosecond pulsed laser and the transient signals were recorded on a Tektronix TDS 3012B oscilloscope.

Cyclic voltammetry

Cyclic voltammetry was performed using a CHI610D Electrochemical workstation (Shanghai, China).Cyclic voltammograms were recorded at scan rates of 100 mV/s. The electrolytic cell used was a three electrodes cell. Electrochemical measurements were performed at RT using 0.1 M tetrabutylammonium hexafluorophosphate (TBAP) as supporting electrolyte, after purging with N_2. The working electrode was a glassy carbon electrode, and the counter electrode was platinum electrode. A non aqueous $Ag/AgNO_3$(0.1 M in acetonitrile) reference electrode was contained in a separate compartment connected to the solution via semipermeable membrane. CH_3CN was used as the solvent. Ferrocene was added as the internal references.

Aknowledgement

We thank the NSFC (20972024, 21273028, 21421005 and 21473020), the Royal Society (UK) and NSFC (China-UK Cost-Share Science Networks, 21011130154), and Ministry of Education (SRFDP-20120041130005) Program for Changjiang Scholars and Innovative Research Team in University [IRT_13R06], the Fundamental Research Funds for the Central Universities (DUT14ZD226) and Dalian University of Technology (DUT2013TB07) for financial support.

Notes and references

State Key Laboratory of Fine Chemical, School of Chemical Engineering, Dalian University of Technology, Dalian, 116024, P.R. China. Fax: (+86) 411-8498-6236; E-mail: zhaojzh@dlut.edu.cn;
Web: http://finechem.dlut.edu.cn/photochem;

† Electronic Supplementary Information (ESI) available: molecular structure characterization data, UV/Vis absorption and emission spectra, time-resolved transient absorption spectroscopy and DFT calculations. See DOI: 10.1039/b000000x/

1 B. F. DiSalle and S. Bernhard, *J. Am. Chem. Soc*., 2011, **133**, 11819–11821.
2 (*a*) M. Kobayashi, S. Masaoka and K. Sakai, *Angew. Chem. Int. Ed*., 2012, **51**, 7431–7434; (*b*) S. Jasimuddin, T. Yamada, K. Fukuju, J. Otsuki and K. Sakai, *Chem. Commun*., 2010, **46**, 8466–8468.
3 (*a*) D. Nolan, B. Gil, F. A. Murphy, S. M. Draper, *Eur. J. Inorg. Chem.*, 2011, 3248–3256; (*b*) D. Nolan, B. Gil, L. Wang, J. Zhao, S. M. Draper, *Chem. Eur. J.*, 2013, **19**, 15615–15626.
4 X. Wang, S. Goeb, Z. Ji, N. A. Pogulaichenko and F. N. Castellano, *Inorg. Chem*., 2011, **50**, 705–707.
5 S. Erbas-Cakmak and E. U. Akkaya, *Angew. Chem. Int. Ed*., 2013, **52**, 11364–11368.
6 (*a*) S. Erbas-Cakmak, O. A. Bozdemir, Y. Cakmak and E. U. Akkaya, *Chem. Sci*., 2013, **4**, 858–862; (*b*) E. Deniz, G. C. Isbasar, Ö A. Bozdemir, L. T. Yildirim, A. Siemiarczuk, and E. U. Akkaya, *Org. Lett.*, 2008, **10**, 3401–3403.
7 T. N. Singh-Rachford and F. N. Castellano, *Coord. Chem. Rev*., 2010, **254**, 2560–2573.
8 J. Zhao, S. Ji and Huimin Guo, *RSC Adv*., 2011, **1**, 937–950.
9 P. Ceroni, *Chem. Eur. J*., 2011, **17**, 9560–9564.
10 (*a*) A. Monguzzi, R. Tubino, S. Hoseinkhani, M. Campione and F. Meinardi, *Phys. Chem. Chem. Phys*., 2012, **14**, 4322–4332. (*b*) Y. C. Simon and C. Weder, *J. Mater. Chem*., 2012, **22**, 20817–20830.
11 J. Peng, X. Jiang, X. Guo, D. Zhao, Y. Ma. *Chem. Commun.*, 2014, **50**, 7828–7830.
12 J. Zhao, W. Wan, J. Sun and S. Guo, *Chem. Soc. Rev*., 2013, **42**, 5323–5351.

13 (*a*) J. Fan, M. Hu, P. Zhan, X. Peng, *Chem. Soc. Rev.*, 2013, **42**, 29–43; (*b*) Y. Chen, L. Wan, X. Yu, W. Li, Y. Bian, J. Jiang. *Org. Lett.*, 2011, **13**, 5774–5777; (*c*) D. Hablot, A. Harriman and R. Ziessel, *Angew. Chem. Int. Ed.*, 2011, **50**, 7833–7836; (*d*) N. Armaroli, J.-F. Eckert, J.-F. Nierengarten, *Chem. Commun.,* 2000, 2105; (*e*) R. Bandichhor, A. D. Petrescu, A.Vespa, A. B. Kier, F. Schroeder, K. Burgess, *J. Am. Chem. Soc.*, 2006, **128**, 10688–10689; (*f*) W. Lin, L. Yuan, Z. Cao, Y. Feng, J. Song, *Angew. Chem. Int. Ed.*, 2010, **49**, 375–379; (*g*) A. P. de Silva, H. Q. N. Gunaratne, T. Gunnlaugsson, A. J. M. Huxley, C. P. McCoy, J. T. Rademacher and T. E. Rice, *Chem. Rev*., 1997, **97**, 1515−1566;

14 (*a*) A. Loudet and K, Burgess, *Chem. Rev*., 2007, **107**, 4891–4932; (*b*) X. Chen, Y. Zhou, X. Peng and J. Yoon, *Chem. Soc. Rev*., 2010, **39**, 2120–2135.

15 15 (*a*) J.-H. Ye, J. Xu, H. Chen, Y. Bai, W. Zhang, W, He, *RSC Adv.*, 2014, **4**, 6691–6695; (*b*) L. Qiu, C. Zhu, H. Chen, M. Hu, W. He, Z. Guo, *Chem. Commun.*, 2014, **50**, 4631–4634; (*c*) A. Roy, D. Kand, T. Saha, P.Talukdar, *RSC Adv*., 2014, **4**, 33890–33896; (*d*) A. Roy, D. Kand, T. Saha, P. Talukdar; *Chem. Commun.*, 2014, **50**, 5510–5513; (*e*) T. Saha, D. Kand, P. Talukdar; *Org. Biomol. Chem.*, 2013, **11**, 8166–8170; (*f*) Z. Chen, D. Wu, X. Han, J. Liang, J. Yin, G.-A. Yu, S. H. Liu. *Chem. Commun.*, 2014, **50**, 11033–11035; (*g*) J. Yin, Y. Kwon, D. Kim, D. Lee, G. Kim, Ying Hu, J.-H. Ryu, J. Yoon, *J. Am. Chem. Soc.*, 2014, **136**, 5351−5358; (*h*) Y. Wu, Y. Xie, Q. Zhang, H. Tian, W. Zhu, A. D. Q. Li, *Angew. Chem. Int. Ed.*, 2014, **53**, 2090–2094.

16 O. A. Bozdemir, S. Erbas-Cakmak, O. O. Ekiz, A. Dana and E. U. Akkaya, *Angew. Chem. Int. Ed*., 2011, **50**, 10907–10912.

17 M. E. El-Khouly, A. N. Amin, M. E. Zandler, S. Fukuzumi and F. D'Souza, *Chem. Eur. J*., 2012, **18**, 5239–5247.

18 (*a*) X. Zhang, Y. Xiao and X. Qian, *Org. Lett*., 2008, **10**, 29–32; (*b*) C.-L. Liu, Y. Chen, D. P. Shelar, C. Li, G. Cheng, W.-F. Fu, *J. Mater. Chem. C*, 2014, **2**, 5471–5478; (*c*) G. Bai, C. Yu, C. Cheng, E. Hao, Y. Wei, X. Mu and L. Jiao. *Org. Biomol. Chem.*, 2014, **12**, 1618–1626.

19 R. Ziessel and A. Harriman, *Chem. Commun*., 2011, **47**, 611–631.

20 S. O. McDonnell, M. J. Hall, L. T. Allen, A. Byrne, W. M. Gallagher and D. F. O'Shea, *J. Am. Chem. Soc*., 2005, **127**, 16360–16361.

21 (*a*) G. Ulrich, R. Ziessel and A. Harriman, *Angew. Chem. Int. Ed*., 2008, **47**, 1184–1201; (*b*) Q. Hao, S. Yu, S. Li, J. Chen, Y. Zeng, T. Yu, G. Yang, Y. Li, *J. Org. Chem.*, 2014, **79**, 459−464; (c) X. Qu, Q. Liu, X. Ji, H. Chen, Z. Zhou, Z. Shen, *Chem. Commun.*, 2012, **48**, 4600–4602.

22 W. Wu, J. Zhao, J. Sun and S. Guo, *J. Org. Chem*., 2012, **77**, 5305−5312.

23 R Ziessel, B. D. Allen, D. B. Rewinska and A. Harriman, *Chem. Eur. J*., 2009, **15**, 7382–7393.

24 Y. Rio, W. Seitz, A. Gouloumis, P. Vázquez, J. L. Sessler, D. M. Guldi and T. Torres, *Chem. Eur. J*., 2010, **16**, 1929–1940.

25 J-Y. Liu, M. E. El-Khouly, S. Fukuzumiand D. K. P. Ng, *Chem. Asian J*., 2011, **6**, 174–179.

26 A. Ciammaichella, P. O. Dral, T. Clark, P. Tagliatesta, M. Sekita and D. M. Guldi, *Chem. Eur. J*., 2012, **18**, 14008–14016.

27 V. Bandi, M. E. El-Khouly, K. Ohkubo, V. N. Nesterov, M. E. Zandler, S. Fukuzumi and F. D'Souza, *Chem. Eur. J*., 2013, **19**, 7221–7230.

28 M. Baruah, W. Qin, C. Flors, J. Hofkens, R. A. L. Vallée,D. Beljonne,M. V. der Auweraer,W. M. De Borggraeve and N. Boens, *J. Phys. Chem. A*., 2006, **110**, 5998–6009.

28 L. Huang, X. Cui, B. Therrien and J. Zhao, *Chem. Eur. J*., 2013, **19**, 17472–17482.

29 X. Qu, Q. Liu, X. Ji, H. Chen, Z. Zhou and Zhen Shen, *Chem. Commun*., 2012, **48**, 4600–4602.

30 C. Zhang, J. Zhao, S. Wu, Z. Wang, W. Wu, J. Ma, S. Guo and L. Huang, *J. Am. Chem. Soc*., 2013, **135**, 10566−10578.

31 S. Guo, L Ma, J. Zhao, B. Küçüköz, A. Karatay, M. Hayvali, H. G. Yaglioglu and A. Elmali, *Chem. Sci*., 2014, **5**, 489–500.

32 Z. Kostereli, T. Ozdemir, O. Buyukcakir, and E. U. Akkaya, *Org. Lett*., 2012, **14**, 3636–3639.

33 Y. Liu and J. Zhao, *Chem. Commun*., 2012, **48**, 3751–3753.

34 L. Huang, X. Yu, W. Wu and J. Zhao, *Org. Lett*., 2012, **14**, 2594–2597.

35 S. Takizawa, R. Aboshi and S. Murata, *Photochem. Photobiol. Sci*., 2011, **10**, 895–903.

36 N. Adarsh, M. Shanmugasundaram, R. R. Avirah and D. Ramaiah, *Chem. Eur. J*., 2012, **18**, 12655–12662.

37 J. Sun, J. Zhao, H. Guo and W. Wu, *Chem. Commun*., 2012, **48**, 4169–4171.

38 (*a*) Z. E. X. Dance, S. M. Mickley, T. M. Wilson, A. B. Ricks, A. M. Scott, M. A. Ratner and M. R. Wasielewski, *J. Phys. Chem. A*, 2008, **112**, 4194–4201; (*b*) B P. Karsten, R K. M. Bouwer, J C. Hummelen, R M. Williams and R A. J. Janssen, *Photochem. Photobiol. Sci.*, 2010, **9**, 1055–1065; (c) D. Veldman, S. M. A. Chopin, S. C. J. Meskers, and R.A. J. Janssen, *J. Phys. Chem. A*, 2008, **112**, 8617–8632; (*d*) M. Murakami, K. Ohkubo, P. Mandal, T. Ganguly, S. Fukuzumi, *J. Phys. Chem. A* 2008, **112**, 635–642.

Graphical Abstract:

Switch the triplet excited state of the C_{60}-dimethyl-aminostyryl bodipy dyads/triads

Ling Huang and Jianzhang Zhao*

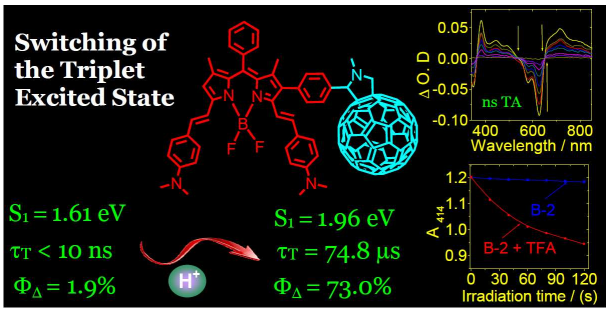

Switching of the triplet excited state of Bodipy-C_{60} dyads/triads with acid/base was studied with nanosecond time-resolved transient difference absorption spectroscopy.